Geophys. J. Int. (1996) **125**, 504–518

A lithospheric cross-section through the Swiss Alps—I. Thermokinematic modelling of the Neoalpine orogeny

N. Okaya,* R. Freeman, E. Kissling and St. Mueller
Institute of Geophysics, ETH Zurich, ETH Hoenggerberg, CH-8093 Zurich, Switzerland

Accepted 1995 December 29. Received 1995 December 29; in original form 1995 January 4

SUMMARY

In this paper we develop a forward 2-D thermokinematic model to investigate the Neoalpine 35–0 Ma phase of orogeny along the European Geotraverse (EGT) through the Swiss Alps on a crustal and lithospheric scale. Using a divergence-free kinematic model (div $\mathbf{v} = 0$), we define mass displacements, which subsequently serve as input to a transient thermal model. The thermal model uses critically assessed material parameters and accounts for the depth dependence of the thermal properties in processes such as crustal thickening and mantle–lithospheric subduction. Based on the present-day density pattern of the deep seismic image and estimated exhumation and shortening rates, we derive, in a first modelling step, a mass-displacement field describing the Neoalpine orogeny as a uniform process in time. In a second—thermal—modelling step, this kinematic scenario is further refined by modelling the non-uniform cooling histories of the southern Lepontine in the Penninic domain. For that purpose we adopt lithospheric shortening rates—and consequently exhumation rates—to agree with total Neoalpine shortening, while keeping the geometry of the kinematic model fixed. The resultant thermokinematic model reflects the main characteristics of Neoalpine tectonics, and shows a good overall agreement with combined geological and geophysical data. The asymmetric feature of the present-day tectonic structure along the profile is strongly reflected in the thermal structure of the lithosphere. This demonstrates the need for a kinematic model to investigate the deep-temperature field in active tectonic provinces. For further refinement of the model, the amounts of shortening have to be more precisely estimated, and a higher spatial density in geochronological and metamorphic data is required. Furthermore, surface heat-flow values are, up to now, too uncertain to constrain the predicted surface heat flow. In summary, our results show that we need, in particular, data constraining the horizontal component of the tectonic and thermal evolution. The results of the Neoalpine orogeny modelling demonstrate that the presented thermokinematic procedure yields a good first-order approximation to investigate crustal-scale and lithospheric processes. We conclude, therefore, that the approach presented provides the potential for application not only to continent–continent collision zones, but also to any active tectonic province.

Key words: collision belts, crustal deformation, European Geotraverse, lithosphere, Swiss Alps.

1 INTRODUCTION

This is the first of two papers investigating the thermomechanical structure of the lithosphere along the European Geotraverse (EGT) (Blundell, Freeman & Mueller 1992) through the Swiss Alps. In part I (this paper) the thermal structure of the lithosphere along the profile is calculated, based on a 2-D transient thermokinematic model (Okaya 1993) consistent with large-scale geological and geophysical observations. In part II we use the resulting present-day temperature field to study aspects related to the mechanical structure down to the depth of the lower lithosphere on the basis of strength envelopes (Okaya, Cloetingh & Mueller 1996).

The Alps represent a relatively young continent–continent collision zone, which started its evolution during the Mesozoic

* Now at: Institute of Geophysics, FU Berlin, Malteserstrasse 74-100, Haus D, D-12249 Berlin, Germany.

collapse of the Variscan orogen with rift-related extension. At about 92 Ma this period was followed by the main compressional episodes of the Alpine orogeny, due to rifting in the central Atlantic: the Cretaceous Eoalpine phase, and the Tertiary Meso- and Neoalpine phases (e.g. Trümpy 1973, 1982). The geometry of the tectonic structure is well constrained (Fig. 1). A detailed image of the deep structure along a N–S profile crossing the central Alps perpendicular to strike (Ansorge *et al.* 1991; Valasek *et al.* 1991; Ye 1992; Ye *et al.* 1990) was obtained recently in the framework of the European Geotraverse (EGT) project (Blundell *et al.* 1992). This provides new and important constraints for possible models of orogenic evolution (Figs 1 and 2). The still-active lithospheric deformation causes a perturbation of the thermal and mechanical structures which are key parameters for understanding the geodynamics of this continent–continent collision zone.

In the 1970s, thermal models of the Alps were restricted to determining crustal temperatures using a steady-state approach (Giese 1970; Buntebarth 1973; Rybach *et al.* 1977). These models derived the lateral change in the temperature–depth distribution from a spatial variation in radiogenic heat production and thermal conductivity. However, steady-state thermal models assume that the Alps are tectonically stable and in thermal equilibrium. Present-day uplift rates (e.g. Greiger, Kahle & Gubler 1986; Gubler *et al.* 1992) and seismic and neotectonic activity (e.g. Pavoni 1980; Deichmann & Rybach 1989; Deichmann & Baer 1990) document that the Alps are still tectonically active today. Davy & Gillet (1986) considered the transient effects of tectonic activity by assuming that tectonic mass displacements occur instantaneously. They calculated temperatures in a 1-D transient thermal-conduction model with constant radiogenic heat production and thermal conductivity. A further improvement was accomplished in 1-D transient models, which, besides heat conduction and radiogenic heat production, take into account heat convection due to vertical mass displacements (Werner *et al.* 1976; Werner 1980, 1981; Bradbury & Nolen-Hoeksema 1985). Werner (1986) calculated first-order models of the spatially differentiated uplift history of the Alps by considering laterally differentiated block uplift in a 2-D transient model. However, these models describe only the uplift history and not the whole mountain-building process, which is a collage of crustal shortening, thickening and uplift, as well as subduction of mantle lithosphere. In a first attempt these processes were considered by

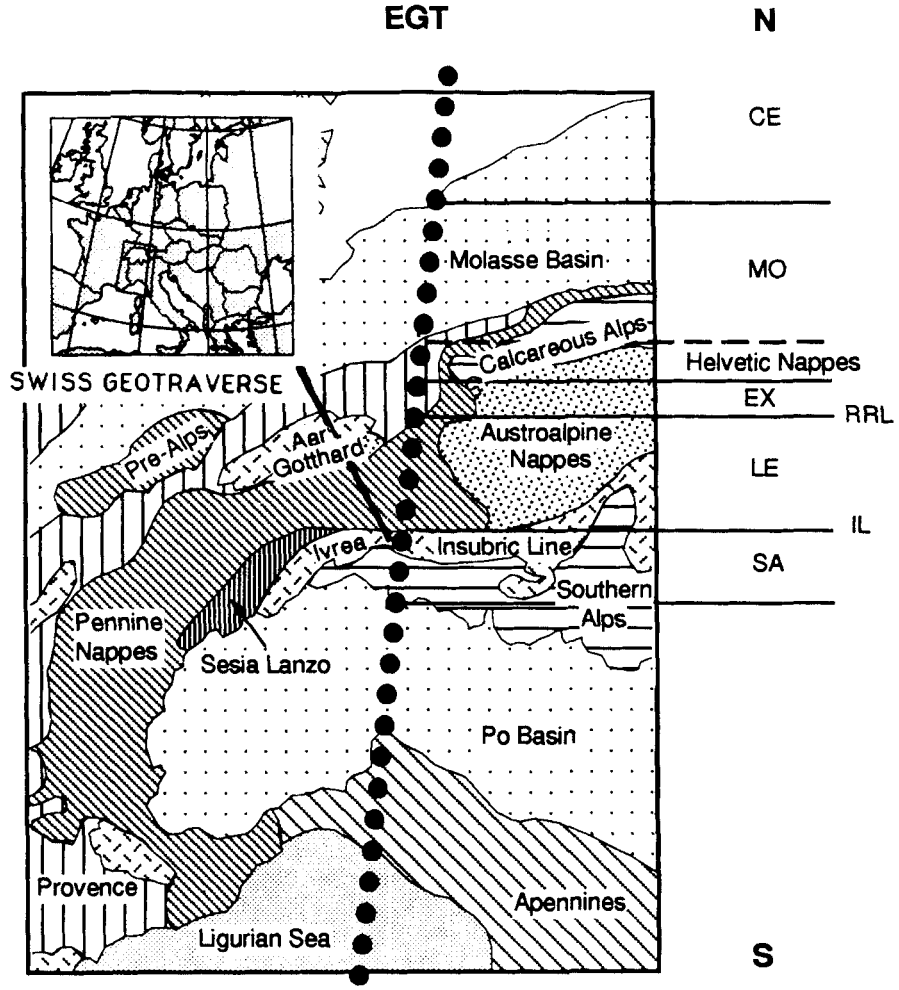

Figure 1. Tectonic map of the Central and Western Alps (after Coward & Dietrich 1989) showing the location of the European Geotraverse (EGT), the location of the Swiss Geotraverse, and the tectonic units accounted for in the thermokinematic model (MO: Molasse Basin; EX: External Massifs; RRL: Rhine–Rhone line; LE: Lepontine of the Penninic domain; IL: Insubric Line; SA: Southern Alps). CE refers to the central European structure (see Fig. 2b).

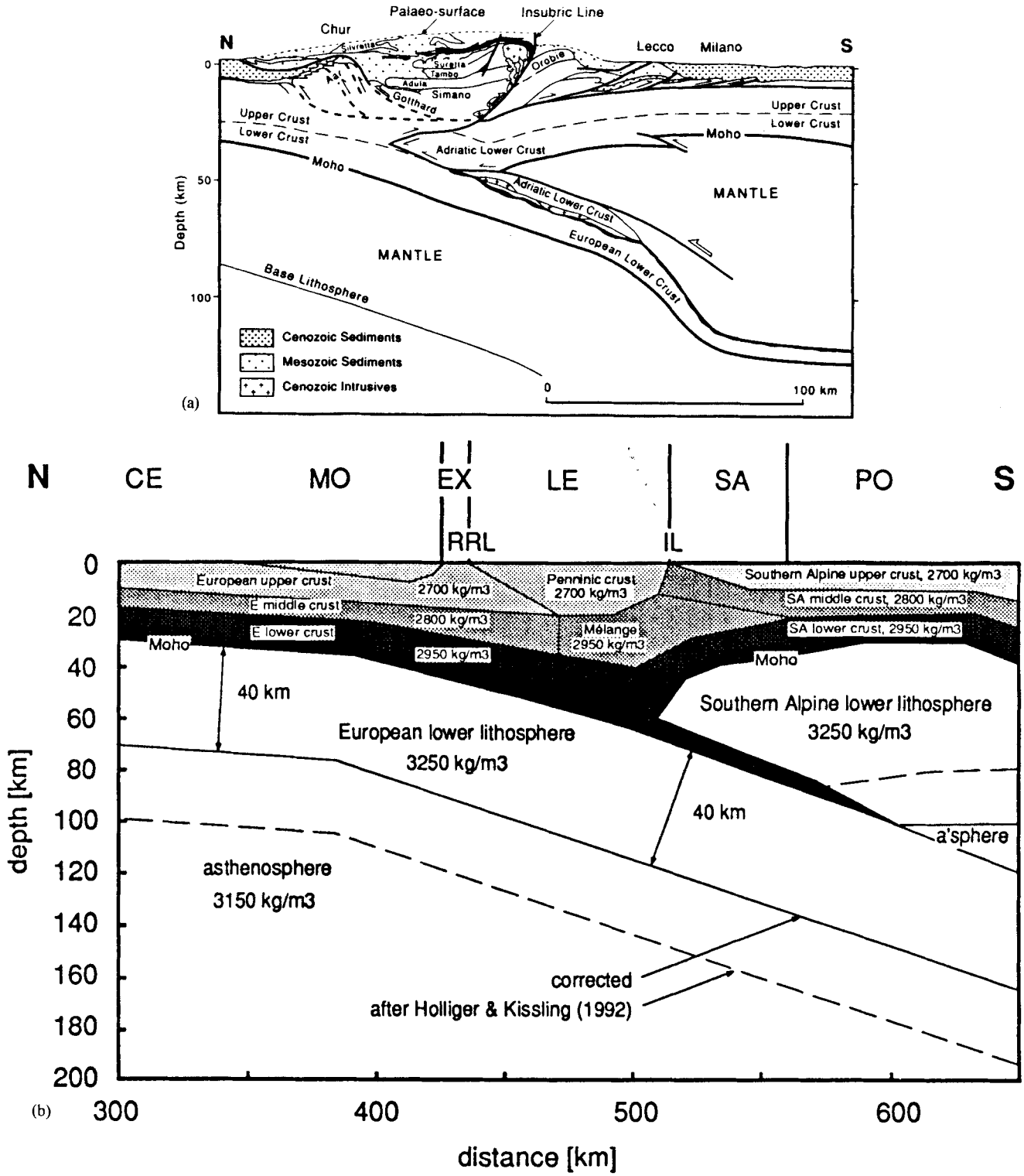

Figure 2. Crustal cross-section between the Molasse Basin in the north and the Po Basin in the south. (a) Geological cross-section of the Alpine lithosphere beneath the European Geotraverse (EGT), based on seismic near-vertical reflection and refraction profiling (after Pfiffner 1992). (b) Gravity interpretation along the EGT through the Swiss Alps (after Holliger & Kissling 1992). CE refers to the generalized central European structure, for which we assumed a crustal thickness of 30 km and a lithospheric thickness of 70 ± 10 km (Panza *et al.* 1980; Suhadolc *et al.* 1990), indicated by the dashed line. The central European crust is assumed to consist of an upper, middle and lower crust, each of 10 km thickness. The thickness of the lithospheric mantle is corrected to 40 km, according to central European conditions. For MO, EX, LE and SA see Fig. 1.

Kissling, Mueller & Werner (1983) and Werner & Kissling (1985) using a symmetric, strongly schematized mass-displacement field. The models of the Alpine orogeny mentioned above confirm that in tectonically active zones the convective heat due to tectonic mass displacements is fundamental in investigating the thermal structure of the lithosphere.

Since the publications of Kissling *et al.* (1983) and Werner & Kissling (1985), the asymmetric nature of Alpine collisional tectonics has been firmly established by seismic profiling in the framework of the Swiss National Science Foundation Program 20 (NFP20) (Valasek *et al.* 1991) and the European Geotraverse Project (EGT) (Blundell *et al.* 1992). The main goal of our modelling effort is to investigate the thermal effects related to mass displacements, which account for the asymmetrical nature of the present-day deep structure beneath the Alps. For this purpose Okaya (1993) developed a new 2-D transient thermokinematic model, which we applied to the 35–0 Ma of the Neoalpine orogeny along the EGT through the Swiss Alps. Our modelling emphasis is put on developing a numerical model to quantify the large-scale thermotectonic characteristics of the Alpine orogen consistent with combined geological and geophysical observations.

2 MODEL DEFINITION AND MODELLING PROCEDURE

To investigate the present-day thermal structure along the European Geotraverse (EGT) through the Swiss Alps (Figs 1 and 2) we restrict our model of Alpine evolution to the last tectonothermal event, i.e. the 35–0 Ma phase of the Neoalpine orogeny. Most authors place the beginning of this phase at the climax of the Tertiary metamorphic event at about 40–35 Ma (Frey *et al.* 1980; Hunziker, Desmons & Martinotti 1989). This phase is constrained by thermal and tectonic data, such as palaeotemperature data, surface heat flow, amounts of crustal shortening, metamorphic grade and deep seismic structure. These provide a good basis upon which to constrain and test the thermokinematic model.

Additionally, the obviously 3-D problem is simplified by considering only the central Alps. The 2-D modelling approach adopted here assumes that the main direction of mass displacement takes place in the chosen cross-sectional plane. Furthermore, variations in vertical movements perpendicular to the plane should be negligible to guarantee no temperature change in the profile plane due to lateral heat flow. For the Neoalpine phase, the relative motion between Africa and Europe shows mainly a N–S component (Dewey *et al.* 1989), coinciding roughly with the orientation of the EGT (Fig. 1). A significant deviation—about 315° NW—is recorded for the time period from 10–0 Ma (Dewey *et al.* 1989). This component is mainly compensated farther to the west by the formation of the Jura mountains and shows a negligible effect in the shortening of the Subalpine Molasse (Burkhard 1990) along the EGT.

Clearly, the Eo- and Mesoalpine lithosphere was not in thermal equilibrium and was strongly influenced by the earlier phases of Jurassic–Cretaceous rifting and subsequent compression with oceanic subduction. However, in this paper we focus on building up a model with which to calculate the thermal effects of the continental collision phase only. For this purpose we suppose that the model is initially (35 Ma) in tectonic and thermal equilibrium, represented by a lithosphere–asthenosphere system that is similar to the present-day central European structure (CE in Fig. 2b). We render the assumed stable tectonic initial conditions by a flat crust–mantle structure (CE in Fig. 2b) and, consequently, model the lithospheric mantle and crustal roots under the Swiss Alps as being created during Neoalpine deformation.

Starting at 35 Ma, the Neoalpine orogeny is tuned step by step to the observations. In the first step the large-scale tectonic mass-displacement field is modelled using a 2-D kinematic model (Okaya 1993). The geometry of the mass-displacement field is derived from the pattern of the present-day deep structure (Fig. 2). Quantification of the mass-displacement field is based on estimates of total Neoalpine exhumation and upper-crustal shortening. These data are combined with plate-tectonic principles to derive a lithospheric mass-displacement field. The resultant mass-displacement field is then tested against the input data by tracking the deformation of an initially flat-layered reference structure through time and comparing it to the present-day deep lithospheric structure. The derived velocity field serves as input to a 2-D transient thermal model (Okaya 1993). In this second thermal modelling step the mass-displacement field is so adapted that the cooling histories of rock samples cropping out in the southern Lepontine are fitted. The results are compared to present-day uplift rates and surface heat flow along the profile.

3 KINEMATIC MODEL

The objective of the kinematic model (Okaya 1993) is to describe numerically complex tectonic mass displacements as they are documented in continent–continent collisional zones, and other tectonically active areas. The fundamental idea of the mathematical description is based on the theorem of vector addition. According to this theorem, complex velocity fields are built up by superposing simple velocity fields which are referred to as 'velocity elements'. Mass conservation is guaranteed by using a divergence-free ($\operatorname{div} \mathbf{v} = 0$) analytical description for the velocity elements.

The velocity elements describe mass flow in L-shaped vertical and sub-vertical channel systems (Fig. 3a). Using a vertical channel system, a 90° change in direction of mass flow is obtained. A change in mass flow by any angle $]0°, 180°[$ is achieved via a subvertical channel system. Inside the channel system the mass flow is a combination of block displacement, simple shear and general deformation (Fig. 3b). The horizontal and vertical channels are split into three areas: a central domain of block displacement bordered by domains of simple shear. The region connecting the horizontal and (sub)vertical channels is characterized by general deformation. The widths of the areas of block displacement and simple shear can be freely chosen, whereas the dimension of the area of general deformation follows. The velocity elements described above can be freely arranged and superposed in the profile window to model any redistribution of mass volumes (Fig. 3c). Thus complex tectonic mass displacements can be built up successively.

4 LARGE-SCALE TECTONIC MASS DISPLACEMENTS IN THE NEOALPINE OROGENY

The Neoalpine orogeny is characterized by tectonic exhumation and thickening due to the continuous convergence of the

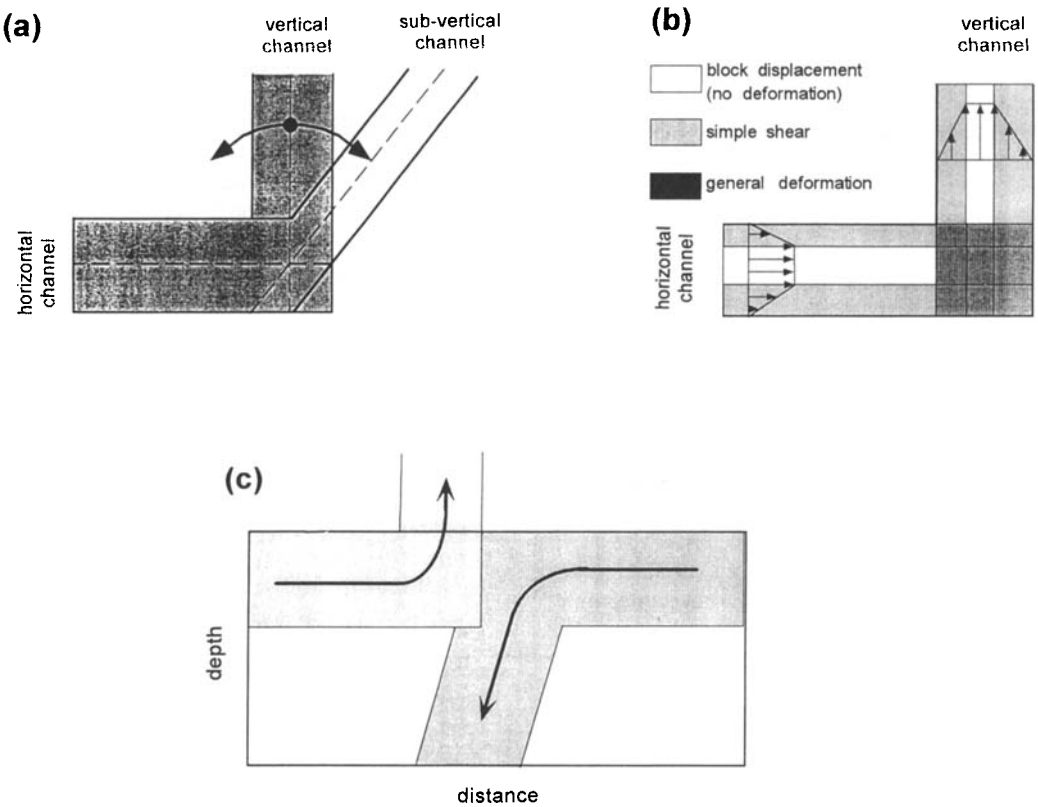

Figure 3. (a) Channel geometry of velocity elements. (b) Strain distribution of the mass flow within the channel system. (c) Schematic example illustrating the use of velocity elements to build up complex tectonic mass-displacements fields.

European plate and the Adriatic promontory (Channell, D'Argenio & Horváth 1979) of the African plate. In a first modelling step we assume that the Neoalpine orogeny can be described by a constant tectonic mass-displacement field describing the last 35 Ma as a uniform tectonic process. For this purpose we extrapolate the implications of the present-day large-scale tectonics back into the geological past.

The density distribution of the present-day deep-crustal structure beneath the Alps (Fig. 2b) provides the basis upon which the geometry of the Neoalpine tectonic mass-displacement field is modelled. The large-scale tectonic features are the southward subduction of the European lithospheric mantle beneath the Adriatic plate, the northward wedging of the Adriatic plate into the European plate, the asymmetric crustal root, and the N–S asymmetric crustal exhumation with a maximum tectonic uplift reached in the southern Lepontine ('palaeo-surface' in Fig. 2a). The asymmetric Moho beneath the Alps and the asymmetric exhumation is interpreted as resulting from intracrustal tectonic wedging (Mueller 1990). The development of the Molasse and Po Basins as such is not included in the kinematic model. However, under the Molasse Basin and the Southern Alps we consider, as a kinematic feature, the downward flexure of the European and Adriatic lithospheric plates due to loading by (sub)surface loads.

Quantification of the mass displacements is based on estimates of total Neoalpine exhumation and upper-crustal shortening. Exhumation depths are derived from metamorphic data (Frey *et al.* 1980), which yield an estimate of the total vertical displacement since the last major metamorphic event at about 35 Ma (Hunziker *et al.* 1989; Hurford, Flisch & Jäger 1989). The metamorphic pressures (Fig. 4a) are rendered depths using a standard lithostatic pressure–depth relation (e.g. Thompson 1992). The resultant total exhumation is shown in Fig. 4(a). The total amount of Neoalpine shortening (Fig. 4b), for the entire Alpine area, was estimated from structural-geological data as about 200 km (Laubscher 1991), with shortening of 145–150 km north of the Insubric Line on the European side (Laubscher 1991; Pfiffner 1992) and 50 km south of the Insubric Line in the region of the Southern Alps (Laubscher 1991; Schoenborn 1992). An estimated 25–30 km of the northern shortening is compensated in the area of the External Massifs and the remaining 125–130 km in the Lepontine. Exhumation depths (implying vertical mass flow) in combination with crustal shortening (representing horizontal mass flow) give the position of the present-day surface at 35 Ma and define the Neoalpine exhumation volume (Fig. 4c).

To constrain the Neoalpine mass-displacement field on a lithospheric scale, the data summarized above are combined with plate-tectonic principles, as illustrated in Fig. 5. Away from the collision zone, the lithosphere shortens at a constant rate over the entire lithospheric thickness (i.e. rigid push). Within the actual collision zone only subduction of the denser mantle lithosphere occurs. This assumption is reasonable for the Neoalpine orogeny as there was no or negligible conversion of subducted crustal into mantle material (Laubscher 1990). The base of the lithosphere, i.e. the depth at which material begins to partially melt, is assumed to equal the depth at which the movement of the lithospheric plate decouples from

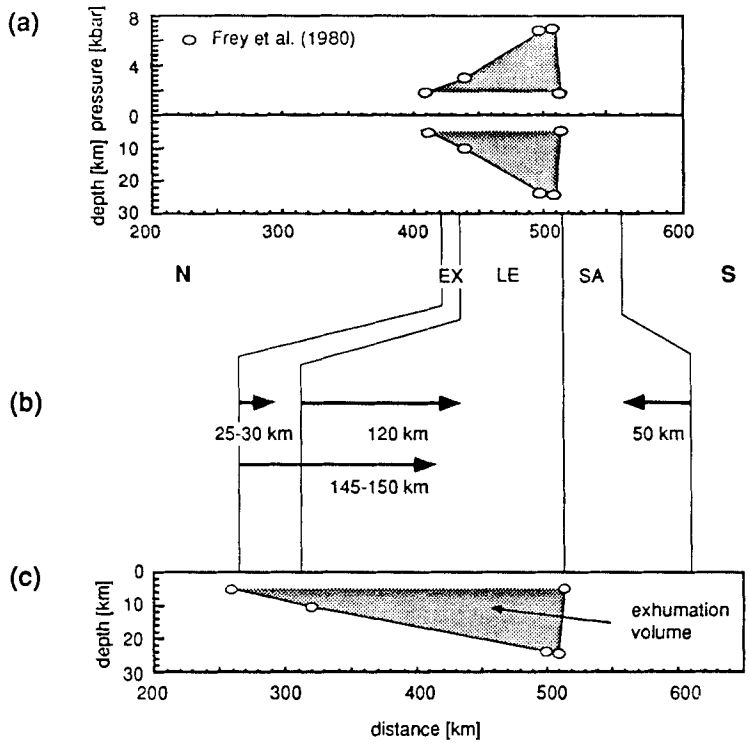

Figure 4. Data base used to quantify the Neoalpine (35–0 Ma) large-scale tectonic mass-displacement field. (a) Pressure conditions of the Tertiary metamorphic event (after Frey *et al.* 1980) (upper panel) and derived exhumation depth (lower panel) used to constrain the average Neoalpine exhumation rate. (b) Amounts of total Neoalpine upper-crustal shortening, as derived from structural geological observations. Northern upper-crustal shortening after Laubscher (1991) and Pfiffner (1992), with shortening in the External Massifs after Pfiffner (1992), and in the Lepontine after Stampfli (1993); southern upper-crustal shortening after Stampfli (1993) and Schoenborn (1992). (c) Compilation of the total Neoalpine exhumation and shortening data used to constrain the Neoalpine exhumation volume.

the mantle convection. Seismic observations document that the base of the lithosphere in central Europe is reached at a depth of 70 ± 10 km (Panza, Mueller & Calcagnile 1980; Suhadolc, Panza & Mueller 1990), whereas there are no reliable constraints on the base of the lithosphere under the central Alps. The base of the lithosphere under the central Alps is obtained by assuming that the Alps developed out of the central European reference structure and that the central European mantle lithosphere subducts by maintaining its thickness. Consequently, along the entire profile we correct the thickness of the mantle lithosphere for the geometry given by the density structure (Holliger & Kissling 1992), to 40 km (dashed line in Fig. 2b).

Based on the data compilation illustrated in Fig. 5 and using the kinematic model (see Section 3), the Neoalpine mass-displacement field is derived (Fig. 6a). Because the vector image is not appropriate to test the modelled mass-displacement field against the observations, the deformation of the flat-layered central European reference structure (CE in Fig. 2b), subject to the defined mass-displacement field, is followed through time. The resultant structure at 0 Ma—after 35 Ma evolution—is displayed in Fig. 6b, in comparison with the density structure (Holliger & Kissling 1992). The result shows good overall agreement between the observed and calculated pattern of the crust–mantle and lithosphere–asthenosphere boundaries. The lithosphere–asthenosphere boundary predicted by the kinematic model reflects a material boundary, and, therefore, cannot be simply compared with the observed base of the lithosphere, which reflects the inception of partial melting, i.e. a thermal boundary. This boundary is further discussed below in the scope of the thermal modelling. Within the crust, the structural development is visualized by plotting the deformed boundaries at initial depths of 0 km, 10 km and 20 km. At mid-crustal depths the 'mélange zone' of Holliger & Kissling (1992), representing material of lower-crustal density at that depth, is largely reproduced by the model. In the upper crust, modelled and observed structures are not comparable, since fault and thrust tectonics at or near the surface are not included in the model. Intracrustal boundaries cropping out in the core of the mountain belt document exhumation of material from greater depth. The amount of exhumation is studied by tracking the present-day surface back in time over the past 35 Ma. A comparison of the observed (Fig. 4c) and predicted position of the present-day surface at 35 Ma is shown in Fig. 7. North of the Insubric Line the predicted exhumation depths disagree with the observed values (Fig. 7a), while the predicted exhumation volume agrees with the reconstructed volume (Fig. 7b). This indicates that the modelled amount of shortening across the External Massifs is slightly too small. The observed jump at the Insubric Line from the highly metamorphic realm of the Lepontine to the non-metamorphic Southern Alps is reproduced approximately by the model.

Since the large-scale tectonic features of the kinematic model show a good overall agreement with the different geological and geophysical observations at hand, the Neoalpine mass-displacement field (Fig. 6a) is, in the following, studied in terms of its effect on lithospheric temperatures.

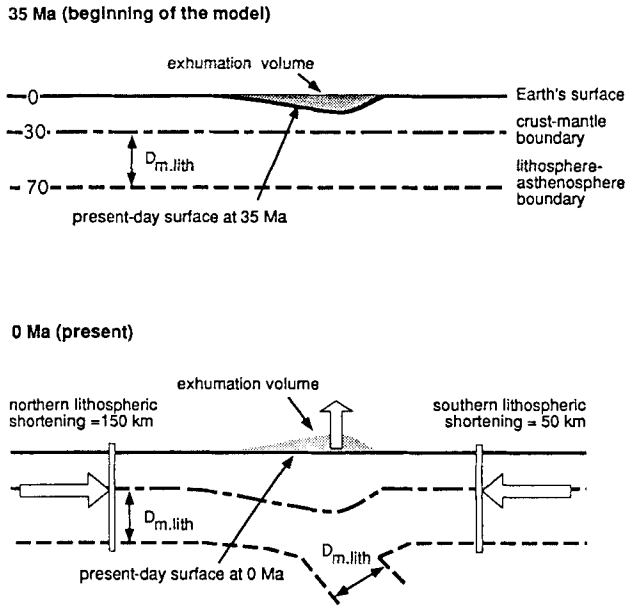

Figure 5. Schematic illustration of how exhumation and shortening data are used to constrain the lithospheric mass-displacement field. The arrows at the right and left sides of the lower panel indicate that outside the deformation area of the Alps we assume a uniform shortening rate over the entire lithospheric thickness. The position of the present-day surface at 35 Ma is given by the line 'surface at 35 Ma', which coincides with the envelope of the exhumation volume shown in Fig. 4(c). D_{lith} indicates the subduction of the entire lithospheric mantle.

5 THERMOKINEMATIC MODEL

Temperatures are calculated on the basis of the transient 2-D heat-transport equation for a moving fluid,

$$\frac{\partial T}{\partial t} = \frac{1}{\rho c_p}\nabla(K\nabla T) + \frac{1}{\rho c_p}A - \mathbf{v}\nabla T + \frac{\alpha g T}{c_p}v_z, \qquad (1)$$

where T is the temperature, t is the time, ρ is the density, c_p is the specific heat capacity, K is the thermal conductivity, A is the radiogenic heat production, $\mathbf{v} = (v_x, v_z)$ is the assumed mass-displacement field, α is the volume expansion coefficient, and g is the acceleration due to gravity. Eq. (1) incorporates the effects of thermal conduction, radiogenic heat production, convection caused by mass displacements, and adiabatic compression, which are all responsible for the temperature distribution on a lithospheric scale.

To account for the depth dependence of the thermal properties, the temperature and depth dependence of the relevant rock parameters are critically assessed and differentiated according to position in the crust, the mantle lithosphere and the sublithospheric mantle (Fig. 8a). Thermal conductivity and specific heat capacity are temperature-dependent. Radiogenic heat production in the crust depends on depth, whereas in the mantle it is constant. Density values are considered constant, but with different values within the crust and within the mantle. The rock parameters are summarized in Appendix A. In addition, the thermal effects of crustal thickening and subduction are accounted for by a 'material updating algorithm' (Fig. 8c). In this algorithm, the crust–mantle boundary is supposed to represent a petrological boundary deforming under the implied mass-displacement field. This assumption is reasonable for the Neoalpine orogeny, as there was no or negligible conversion of crustal into mantle material, and vice versa (Laubscher 1990). The lithosphere–asthenosphere boundary, although migrating with depth due to tectonic movements, is thermally defined as the intersection of the geotherm with the wet solidus of lherzolite (Wyllie 1987). This thermal boundary is determined from the calculated temperature field. Rock parameters are assigned to the actual layer, i.e. crust, mantle lithosphere and sublithospheric mantle, and are updated according to this assignment in each layer at every time step in the numerical integration. In the model, we neglect the development of topography and describe the Earth's surface as a flat top boundary at a depth of 0 km.

Eq. (1) is solved by a finite-difference method for a non-equidistant grid (Peaceman & Rachford 1955). The non-equidistant grid covers an area 1000 km wide and 400 km deep. Grid spacing is 2.5 and 30 km in the vertical and horizontal directions, respectively. The temperatures at the surface and at the bottom boundary are kept fixed at 0 °C and 1600 °C (e.g. Bott 1982), respectively. On the left and right sides of the numerical grid, Neumann boundary conditions ($\partial T/\partial x = 0$) are applied by equating the temperatures to the central European geotherm, which defines the initial condition in the transient thermal calculations.

Initial conditions (Fig. 8b) are calculated using the 1-D stationary heat-conduction equation (notation as in eq. 1),

$$\frac{\partial}{\partial z}\left(K\frac{\partial}{\partial z}T\right) + A = 0, \qquad (2)$$

applied to a reference model for the present central European lithosphere (Fig. 8a). The stationary thermal equation is solved using a numerical finite-difference scheme that accounts for the depth and temperature dependence of the rock parameters. Boundary conditions for the modelling are the surface temperature, taken to be 0 °C, the average central European surface heat flow of 70 ± 10 mW m^{-2} (Cermák *et al.* 1992), and the critical temperature of the olivine α–β spinel phase transition at a depth of 400 km, taken to be 1600 °C (e.g. Bott 1982). As in the transient thermal calculations, the lithosphere–asthenosphere boundary is thermally defined as the intersection of the geotherm with the wet solidus of lherzolite (Wyllie 1987), and is reached in central Europe at a depth of 70–80 km (Panza *et al.* 1980; Suhadolc *et al.* 1990).

In the sublithospheric mantle we ignore the thermally induced mantle convection and simulate temperatures using a thermal conduction model, which considers the sublithosphere to behave purely conductively. This model serves as a far-field bottom-boundary condition and allows us to model the thermokinematic evolution of complex tectonic scenarios down to lower-lithospheric depths. The relevant thermal parameters of a conductive sublithospheric layer are the thermal conductivity and the specific heat capacity. The thermal conductivity is described by a temperature-dependent analytical function (see eq. A3, Appendix A), which is empirically derived such that under steady-state conditions (eq. 1), temperatures in the sublithospheric layer increase nearly adiabatically to a temperature of about 1600 °C at a depth of 400 km. The specific heat capacity in the sublithospheric layer is set artificially high to ensure that the 'steady-state' geotherm for central Europe does not change when input into the 2-D transient calculation. This concept assumes that a tectonically stable area, i.e. the

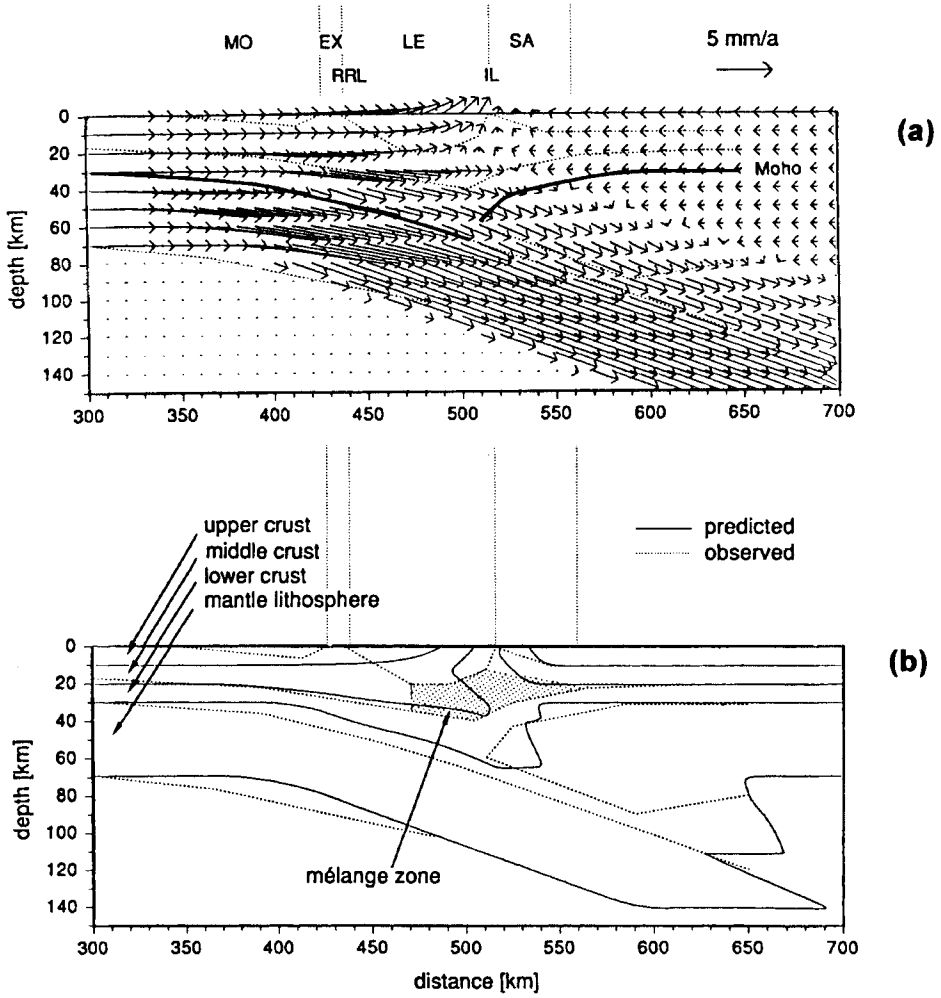

Figure 6. Kinematic modelling results of the Neoalpine (35–0 Ma) orogeny. (a) The assumed large-scale tectonic mass-displacement field along the EGT through the Swiss Alps in comparison with the gravity structure (after Holliger & Kissling 1992) (dotted line) with the crust–mantle boundary shown by a thick line (compare with Fig. 2b). The shaded area under the Southern Alps indicates the wedging geometry. For MO, EX, RRL, LE, IL and SA, see Fig. 1. (b) Tectonokinematic effect of the Neoalpine mass-displacement field showing the deformation of the initially (35 Ma ago) flat-layered central European reference structure (solid line) in comparison with the gravity structure (after Holliger & Kissling 1992) (dotted line) (see Fig. 2b). For MO, EX, RRL, LE, IL and SA, see Fig. 1.

central European lithosphere, is characterized by steady-state thermal conditions down to 400 km depth, and, hence, the base of the lithosphere does not change through time. At the bottom of the lithosphere we could also have chosen a 'film' boundary condition,

$$q = h(T = T_\infty)^n, \tag{3}$$

where q is the surface heat flow, T the temperature, T_∞ the reference temperature of the convecting sublithosphere, and n and h parameters. However, the values of h and n are only poorly known.

6 DEEP THERMAL STRUCTURE ALONG THE EGT THROUGH THE SWISS ALPS

As already mentioned above, the assumed mass-displacement field (Fig. 6a) describes the Neoalpine orogeny as a single uniform process in time. However, it is known from palaeotemperature data that the cooling history of the Lepontine was not uniform (Hurford *et al.* 1989). This problem is tackled in the context of the thermokinematic calculations (Okaya 1993).

Since we are lacking geochronological data along the EGT through the Swiss Alps, we project the cooling histories of the central Lepontine dome along the Swiss Geotraverse (Fig. 1) (Hurford *et al.* 1989) on the EGT. Palaeotemperature data are modelled by tracking the cooling history of rock samples cropping out in the southern Lepontine (Fig. 9a) and by fitting the Neoalpine mass-displacement field to the observed pattern (Fig. 9b). This is accomplished by adjusting lithospheric shortening rates, and, consequently, exhumation rates (Fig. 9c), such that the total shortening agrees with the amount observed, while the geometry of the Neoalpine mass-displacement field is kept fixed. A time stacking of a tectonic phase of fast exhumation lasting from 35 to 20 Ma, followed by a phase of slow exhumation lasting from 20 to 2 Ma and a phase of intermediate exhumation lasting from 2 to 0 Ma produces a cooling pattern in good agreement with the available observations (Hurford *et al.* 1989).

Model results of the last 2 Ma of the Neoalpine orogeny

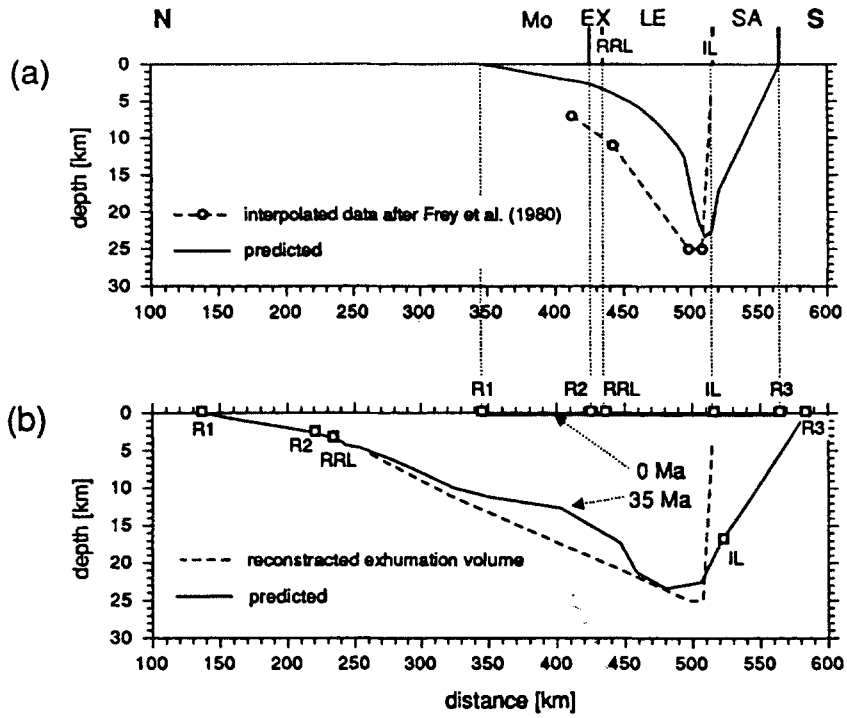

Figure 7. Comparison of the observed (see Fig. 4) and predicted total Neoalpine exhumation depth (a) and exhumation volume (b). In (b) the positions of reference points R1, R2, RRL, IL and R3 are shown to illustrate the effect of the amount of shortening.

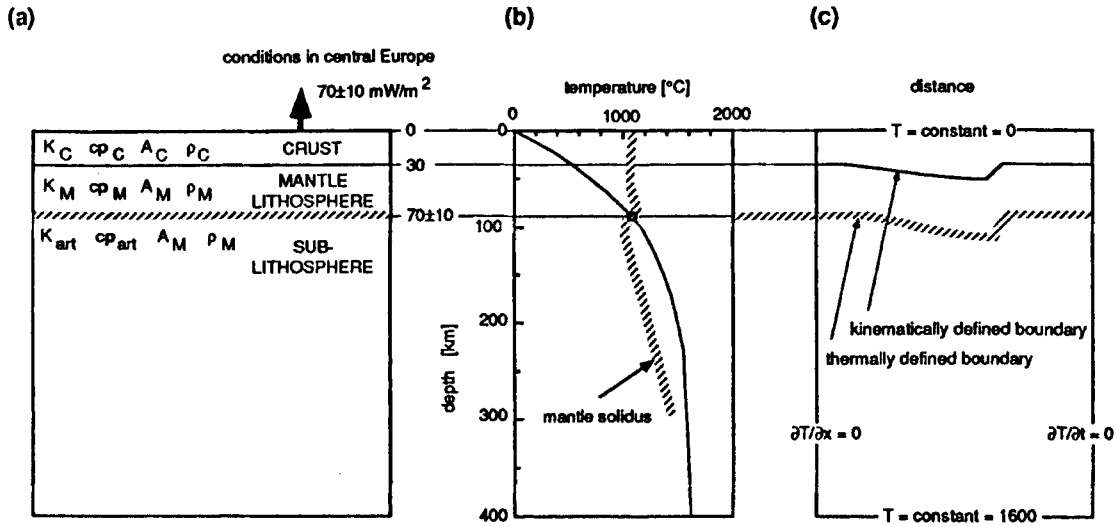

Figure 8. Overview of assumptions and rock parameter setting underlying the transient thermokinematic model. (a) Generalized deep structure and surface heat flow of central Europe serving as a reference model in the transient thermal modelling. Surface heat flow after Cermák *et al.* (1992); deep structure after Panza *et al.* (1980) and Suhadolc *et al.* (1990). K refers to the thermal conductivity, cp to the specific heat capacity, A to the radiogenic heat production and ρ to the density, with subscripts C, M and art refering to the crust, lithospheric mantle and sublithospheric mantle, respectively. (b) Central European geotherm as derived from the steady-state thermal model. The intersection of the geotherm with the solidus of mantle material defines the bottom of the thermal lithosphere and is assumed to coincide with the seismically derived bottom of the lithosphere [compare with (a)]. Solidus of wet lherzolite after Wyllie (1987). (c) Schematic illustration of the 'material updating' algorithm to account for the thermal effects of thickening of the crust and subduction of the lithospheric mantle. See text for description.

yield exhumation rates at the surface which are compared to the pattern of recent uplift rates along the Swiss Geotraverse and the EGT (Gubler 1976, 1991; Gubler *et al.* 1992) (Fig. 10). The calculated uplift rates yield a better agreement with the uplift-rate pattern recorded along the Swiss Geotraverse than along the EGT. A possible explanation is that we used the cooling history of the central Lepontine dome along the Swiss Geotraverse, since, as mentioned above, geochronological data along the EGT are lacking.

For the rock samples cropping out in the southern Lepontine (Fig. 9a) we calculate the corresponding *P–T–t* paths, along with the exhumation histories, i.e. *z–t* paths (Fig. 11). The individual *P–T–t* paths (Fig. 11a) show a change in curvature with time that is correlated to the tectonic phases of fast, slow,

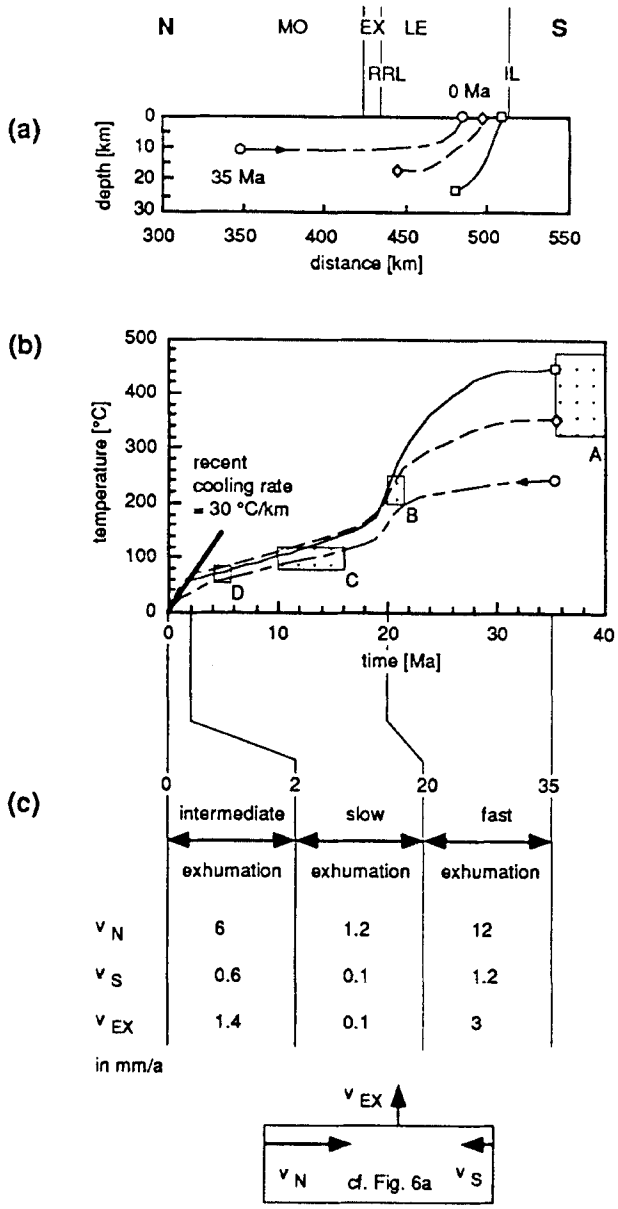

Figure 9. Modelling results of the cooling history of the southern Lepontine. (a) Synthetic trajectories of three rock samples cropping out in the southern Lepontine. The trajectories are calculated on the basis of the assumed Neoalpine mass-displacement field (see Fig. 6a). For MO, EX, RRL, LE, IL and SA, see Fig. 1. (b) Modelled temperature–time paths of three rock samples cropping out in the southern Lepontine [see part (a)] in comparison with the observed palaeotemperature data (after Hurford *et al.* 1989), where box A shows phengite ages from Rb-Sr and K-Ar, box B shows fission-track zircon ages, box C shows fission-track apatite ages and box D shows ages derived from proportions of long (> 10 μm) projected path length. The symbols for the three rock samples are chosen according to (a). (c) Kinematic parameters, which are adapted to fit the observed palaeotemperature data [see part (b)], where v_N is the northern shortening rate, v_S is the southern shortening rate, and v_{EX} is the amplitude of the exhumation rate at the surface.

and intermediate exhumation (Fig. 9c). For the fast exhumation phase (35 Ma to 20 Ma) the different paths of the rock samples are most significant, indicating that the samples come from different thermal regimes. From north to south the curvature of the path changes from concave to convex, whereas the corresponding *z–t* paths exhibit exhumation along a concave path for all rock samples (Fig. 11b). For the slow phase (20 Ma to 2 Ma), where the rock samples are spatially closer together, the *P–T–t* paths show similar curvatures, and for the intermediate phase (2 Ma to 0 Ma) they follow the same geotherm.

To be useful as a constraint on the thermal model, observed surface heat-flow values must be well known and available in a form equivalent to the calculated results. Observed heat-flow values are effected by topography, uplift, palaeoclimate, and ground-water circulation. Along the EGT the corrected heat-flow values still contain the effect of palaeoclimate and ground-water flow, while the calculated heat-flow values include only the effect of uplift. However, comparisons of predicted values with both observed surface heat-flow values (Bodmer & Rybach 1984; Cermák *et al.* 1992)—uncorrected (Fig. 12a) and corrected (Fig. 12b)—show that the predicted surface heat flow is within the range of uncertainty. The large uncertainty in the observed data, both uncorrected and corrected, and the unknown effects of palaeoclimate and ground-water circulation preclude the use of the surface heat flow to constrain the details any further.

The modelled present-day temperature field is shown in Fig. 13, along with the image of the deformed mantle lithosphere (Fig. 6b). The asymmetric characteristics of the tectonic setting are clearly reflected in the deep thermal structure. The horizontal variation in the upper-crustal temperatures follows the gross pattern of the predicted surface heat flow (compare Figs 12 and 13). At mid-crustal levels the 300 °C isotherm shows, from north to south, deformation to greater depth beneath the Molasse Basin and to lesser depth beneath the southern Lepontine. At greater depth, thickening of the lower crust and subduction of the mantle lithosphere lead to a conspicuous deformation of the 400–1100 °C isotherms, reaching a depth of 140 km. The lithosphere–asthenosphere boundary predicted kinematically beneath the Southern Alps deviates from the thermally derived lithosphere–asthenosphere boundary. The thinning of the Southern Alpine mantle lithosphere, as assumed in the density model (Holliger & Kissling 1992) is not reproduced by the kinematic or by the thermal lithosphere–asthenosphere boundary.

The reliability of these results was tested by exploring a number of other thermokinematic models, in which the geometry of the mass displacements was varied (Okaya 1993). These tests demonstrate that the thermokinematic model presented here yields the best agreement with the available data set. The assumed geometry and the physical parameters chosen provide sufficiently good constraints on the upper-lithospheric temperatures but are not sufficient to derive the temperature field in the lower part of the lithosphere.

7 DISCUSSION AND CONCLUSIONS

We have presented a 2-D thermokinematic modelling procedure using the 35–0 Ma phase of Neoalpine orogeny along the EGT through the Swiss Alps as an example. The thermokinematic model quantitatively links tectonic data, i.e. crustal structure, metamorphic data, shortening amounts and uplift rates, to thermal data, i.e. cooling histories and surface heat flow. Our modelling reflects these data in terms of their thermokinematic—or, geophysically speaking, thermotectonic—

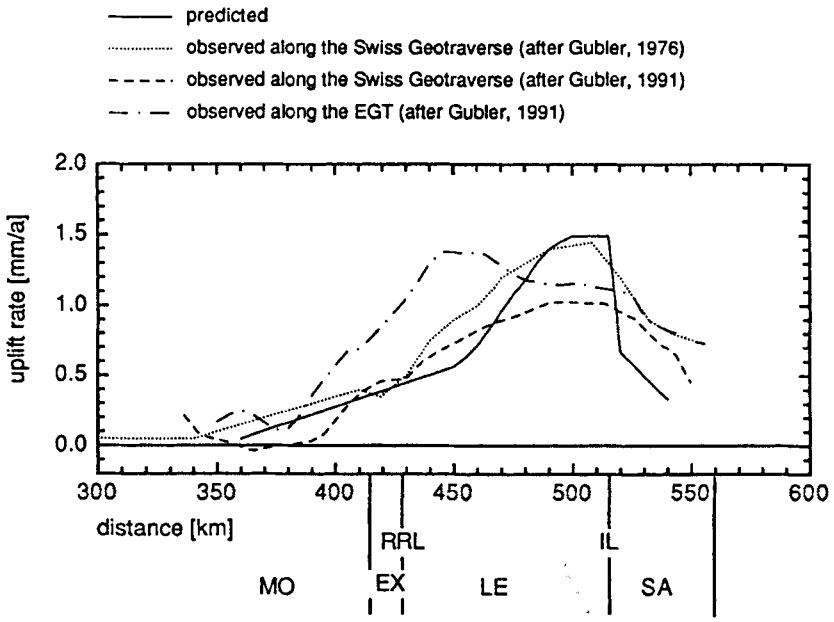

Figure 10. Comparison of the present-day uplift rates, as derived from geodetic observations (Gubler 1976, 1991; Gubler *et al.* 1992) and the exhumation rates at the surface, as given by the kinematic model (see Fig. 6a). For the location of the EGT and the Swiss Geotraverse, see Fig. 1.

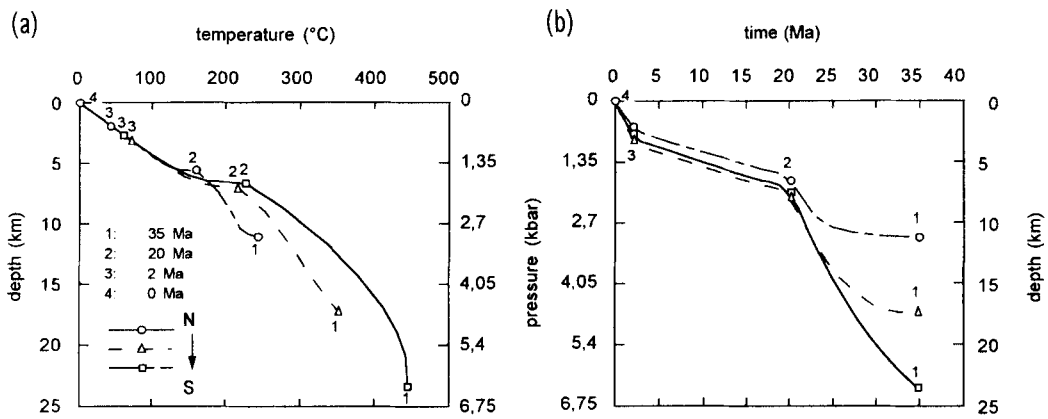

Figure 11. (a) Modelled pressure–temperature–time paths and (b) corresponding exhumation histories of the three rock samples cropping out in the southern Lepontine (see Fig. 9a). The symbols with numbers indicate the times when the mass-displacement field changes (see Fig. 9c).

relationships. The significance of these results, i.e. whether or not they truly represent *the* Neoalpine orogeny, must be considered in light of the assumptions made in the model.

In the thermokinematic modelling we assumed that the model was initially (at 35 Ma) in tectonic and thermal equilibrium. This assumption is obviously an oversimplification. Better initial conditions could be formulated by modelling a pre-history describing the burial history and metamorphic event of the Mesoalpine phase of orogeny. However, as can be seen from the model presented of the Neoalpine orogeny, the value of the model depends on the reliability of the input data. Important pre-suppositions for the thermokinematic procedure are severe constraints on the geometry of the mass displacement field, the magnitude of the mass displacements themselves, the thermal evolution, and the seismic lithosphere–asthenosphere boundary.

For the Alpine kinematic scenario, the basic assumptions are that over the last 35 Ma there were no mass displacements perpendicular to the cross-section and that the tectonic deformation style, i.e. the geometry of the Neoalpine mass-displacement field for the crustal-scale units and the mantle lithosphere (Fig. 6a), remained constant. To model the documented *non-uniform* cooling history of the Lepontine (Hurford *et al.* 1989) we prescribed shortening rates and, in consequence, exhumation rates. In a geodynamic context, this model corresponds to a uniform tectonic style of orogeny, whereas the temporally varying cooling histories are caused by a change in convergence rate of the European and Adriatic plates. One can think of alternative models responsible for a non-uniform cooling history. One possibility would be a change in the tectonic deformation style whilst the relative shortening rate between the European and Adriatic plates remains constant. Another possibility would be that the velocity field at middle- and lower-crustal levels exhibits a much higher spatial variability than modelled here. This would result in a temperature field within the orogenic crust exhibiting strong spatial variations in temperature gradient. In this case, a non-uniform cooling history would result from the effects of the rocks

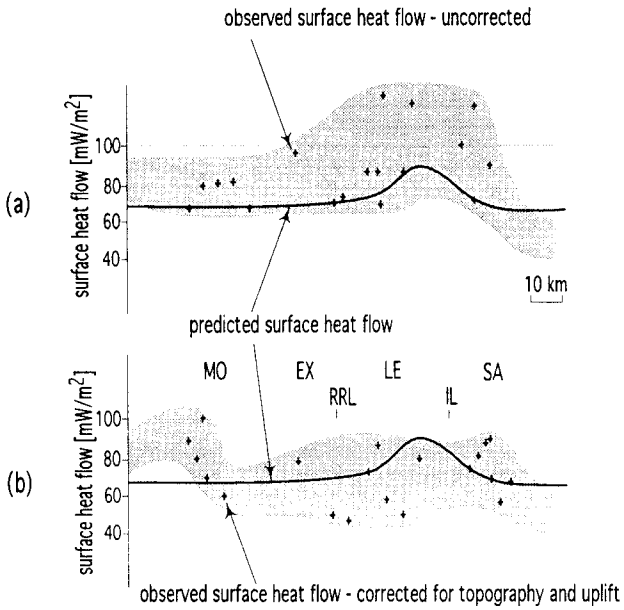

Figure 12. Predicted present-day surface heat flow in comparison with the observed present-day surface heat flow. (a) Uncorrected values; (b) values corrected for uplift and topography. The crosses indicate the data (after Bodmer & Rybach 1984; Cermák *et al.* 1992) and the shaded area gives the range of uncertainty.

moving through thermal provinces varying significantly within the crust. On the basis of the available data and mechanical models (e.g. Bott 1990; Beaumont, Fullsack & Hamilton 1994), it is not possible to tell which mechanism is the most reasonable. Additional quantitative constraints, either from observations or from mechanical modelling, are necessary in order to investigate other tectonic scenarios.

To derive the depth of the base of the lithosphere under the Central Alps we assumed, as did Holliger & Kissling (1992), although this was not clearly stated in their work, that the mantle lithosphere subducts and bends while maintaining its thickness. This seismically 'estimated' base of the lithosphere is only approximately reproduced by the kinematic and thermal models. This might argue in favour of a modification of the kinematic model; however, two facts hold against this. First, the nature of the lithosphere–asthenosphere boundary is still not very well understood, e.g. thermal boundary, mechanical boundary, interaction of the lithospheric and asthenospheric system, and recycling of lithospheric into asthenospheric material and vice versa. Second, the lithosphere–asthenosphere boundary suggested so far shows a sharp angle under the Southern Alps that is characteristic for the deformational behaviour of rigid material. Ductile material would show a rather smooth pattern.

Additionally, we neglected the thermal effect of frictional heat, which might lead to several important effects, such as localized shear heating at thrust faults in the brittle domain of the lithosphere (e.g. Werner 1985; van den Beukel 1989; Molnar & England 1990) and overall viscous heating in the ductile domain. Results obtained by these authors indicate that shear heating might be important locally. To address the relevance of frictional heating to our model these effects have to be explicitly incorporated into the model, whereas a lithospheric-scale model, such as our thermokinematic model, requires the quantification of both shear and viscous heating. For this purpose, a system of faults (and their dynamical evolution), as well as viscosity models, would have to be implemented in the thermokinematic model.

The kinematic modelling results suggest that a refinement of the Neoalpine mass-displacement field (Fig. 6a) could be accomplished by further adjustment of the exhumation pattern and shortening amounts in the region of the External Massifs, the northern Lepontine and the Southern Alps (Fig. 7), and the detailed pattern of the crust–mantle boundary (Fig. 6b), and by including the evolution of the adjacent Molasse Basin in the north and Po Basin in the south of the Alpine belt (Figs 1 and 2). The exhumation depth, derived from metamorphic

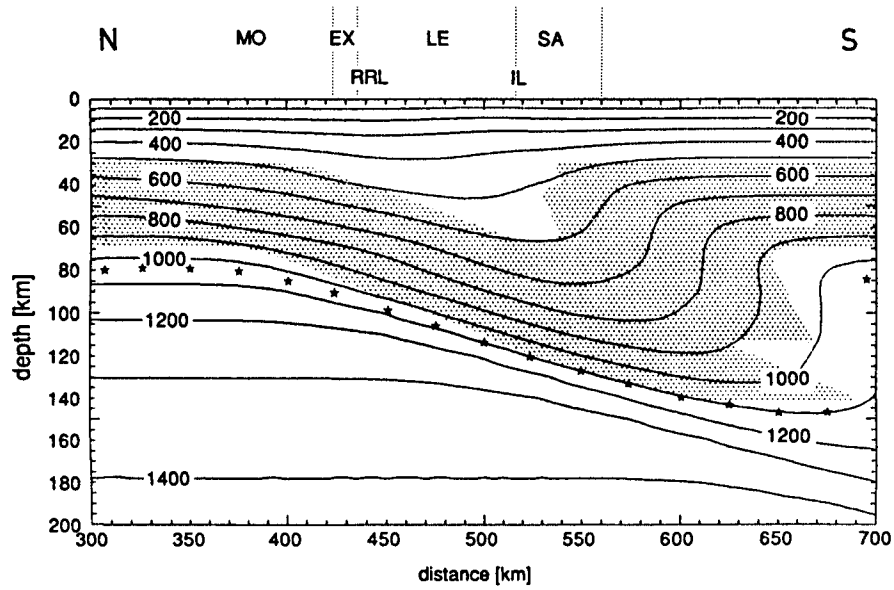

Figure 13. Present-day temperature field (interval between isotherms is 100 °C). The asterisks indicate the lithosphere–asthenosphere boundary, thermally defined as the intersection point of the geotherm with the mantle solidus (see Fig. 8c). The shaded area shows the deformed lithospheric mantle, as derived from the tectonokinematic calculations (see Fig. 6b). For MO, EX, RRL, LE, IL and SA, see Fig. 1.

pressure conditions, and amounts of shortening were used to constrain the mass-displacement field in the crust. These data yield only a few reference points along the profile and were extrapolated over fairly large distances using a linear interpolation (Figs 4 and 5). A higher resolution in metamorphic pressure conditions and a spatial refinement of the amount of shortening along the profile would help to confine the mass-displacement field within the crust. The tracked rock samples exhumed in the southern Lepontine (Fig. 9a) show that, with decreasing distance from the Insubric line, less shortening occurs. This is a characteristic of our kinematic model, which needs to be constrained. However, so far there are no geological data available to affirm or discard this characteristic. Cooling histories and *P–T–t* data contribute only thermal and tectonic information about the vertical component; data on shortening amounts are, so far, too unspecified in time and space.

The thermal results show that the asymmetric feature of the Neoalpine kinematic scenario is strongly reflected in the present-day thermal structure of the lithosphere, demonstrating the need to use a kinematic model to investigate the deep temperature field in an active tectonic province. Within the crust, the resulting present-day temperature gradients (Fig. 13) change dramatically with depth, and laterally through the collision zone. This result is fundamental to the meaning of 'mean' geothermal gradients, which are derived from geochronological data (e.g. Hurford *et al.* 1989). Such 'mean' geothermal gradients do not reflect the 'mean' thermal structure of the crust for a given time during orogeny. A comparison of the cooling histories and the *P–T–t* path shows that the 'mean' geothermal gradient is clearly reflected in the *P–T–t* path (Figs 9b and 11a). Thus, the 'mean' geothermal gradients derived from cooling histories reflect only the thermal structure at the depth where the rocks were residing during this time, and nothing can be said about the horizontal position. A comparison of the predicted and observed surface heat flow (Fig. 12) indicates that the uncertainty of the measured surface heat flow is too large to constrain the modelled surface heat flow. For further comparison, the observed surface heat flow should only be corrected for effects of topography, palaeoclimate and ground-water circulation, while effects of surface uplift and subsidence should not be eliminated. This surface heat flow could give more conclusive constraints on the recent thermal evolution of the Alpine collision zone.

Some important aspects of principal relevance were not addressed in the scope of this modelling, i.e. the sensitivity of the results to the initial temperature field and the reference central European geotherm (Fig. 8b), and the influence of the thermal layering of the lithosphere on mid-lithospheric temperatures (Fig. 8a). These problems are fundamental to quantitative statements on the thermal history and should be investigated in further modelling studies, for which this thermokinematic method offers a flexible tool. Furthermore, an important geodynamic aspect of the modelled mass-displacement field that was not incorporated in the kinematic model is the calculation of the corresponding strain rates and stress field, which could be compared to mechanical-modelling results (e.g. Bott 1990; Beaumont *et al.* 1994).

The overall consistency of the different data in their thermotectonic link indicates that the thermokinematic model presented is a useful tool for displaying an advective temperature field where complex lithospheric- and crustal-scale tectonic processes are significant. Such transient temperature fields could also provide input temperature fields for mechanical and dynamic models (e.g. Beaumont *et al.* 1994; Freeman *et al.* 1995). Furthermore, our results show that, apart from solving principal problems, we need, in particular, data to constrain the horizontal component of the tectonic and thermal evolution. Such data become even more important for 3-D models. The modelling results along the EGT through the Swiss Alps demonstrate the potential of the thermokinematic model for further application to a wide range of relevant questions, not only in continent–continent collision zones, but in any tectonic province where combined thermal and kinematic effects play an important role.

ACKNOWLEDGMENTS

We thank G. Bassi, G. Bertotti, S. Cloetingh, P. Giese, W. Mooney and O. Oncken for useful discussions and suggestions. D. Werner gave the original impetus for this study and also provided algorithms for the thermal calculations. This research was partially supported by the Swiss National Foundation Program 20 'Deep Structure of the Alps' (NFP20), financed by the Schweizerische National Fond. Contribution No. 872, Institute of Geophysics, ETH Zurich, Switzerland.

REFERENCES

Ansorge, J. *et al.*, 1991. Integrated analysis of seismic normal incidence and wide-angle reflection measurements across the eastern Swiss Alps, in *Continental lithosphere: Deep seismic Reflection,* pp. 195–205, eds Meissner, R., Brown, L., Dürbaum, H.-J., Franke, W., Fuchs, K. & Seifert, F., *Am. Geophys. Un., Geodyn. Ser.,* **22.**

Beaumont, C., Fullsack, P. & Hamilton, J., 1994. Styles of crustal deformation in compressional orogens caused by subduction of the underlying lithosphere, *Tectonophysics,* **232,** 119–132.

Blundell, D., Freeman, R. & Mueller, S., 1992. *A Continent Revealed: The European Geotraverse,* Cambridge University Press, Cambridge.

Bodmer, P. & Rybach, L., 1984. Geothermal map of Switzerland: Heat flow density, *Contributions to the Geology of Switzerland, Geophysics Series* **22,** Swiss Geophysical Commission, ETH Zurich.

Bott, M.H.P. (ed), 1982. *The Interior of the Earth: its structure, constitution and evolution,* 2nd edn, Edward Arnold, London.

Bott, M.H.P., 1990. Stress distribution and plate boundary forces associated with collision mountain ranges, *Tectonophysics,* **182,** 193–209.

Bradbury, H.J. & Nolen-Hoeksema, R.C., 1985. The Lepontine Alps as an evolving metamorphic core complex during A-type subduction: evidence from heat flow, mineral cooling ages, and tectonic modeling, *Tectonics,* **4,** 187–211.

Buntebarth, G., 1973. Modellberechnungen zur Temperatur-Tiefen-Verteilung im Bereich der Alpen und des Alpenvorlandes, *Zeitschr. Geophys.,* **39,** 97–107.

Burkhard, M., 1990. Aspects of large-scale Miocene deformation in the most external part of the Swiss Alps (Subalpine Molasse and Jura fold belt), *Eclog. geol. Helv.,* **83,** 559–583.

Cermák, V. & Rybach, L., 1982. Thermal properties, in *Landolt-Börnstein, Numerical Data and Functional Relationships in Science and Technology,* New Ser. V, Vol. 1, Physical Properties of Rocks, A, pp. 305–371, ed. Angenheister, G., Springer-Verlag, Berlin.

Cermák, V., Balling, N., Della Vedova, B., Lucazeau, F., Pasquale, V., Pellis, G., Schulz, R. & Verdoya, M., 1992. Heat-flow density, in *A Continent Revealed: The European Geotraverse, Atlas of Compiled Data,* pp. 3–5, eds Freeman, R. & Mueller, S., Cambridge University Press, Cambridge.

Channell, J.E.T., D'Argenio, B. & Horváth, F., 1979. Adria, the African

promotory, in *Mesozoic Mediterranean paleogeography, Earth Sci. Rev.*, **15,** 213–292.

Chapman, D.S., 1986. Thermal gradients in the continental crust, in *The Nature of the Lower Continental Crust,* pp. 63–70, eds Dawson, J.B., Carswell, D.A. & Wedepohl, K.H., Geol. Soc. Lond. Spec. Publ. **24.**

Chapman, D.S. & Pollack, H.N., 1977. On the regional variation of the heat flow, geotherms, and lithospheric thickness, *Tectonophysics,* **38,** 279–296.

Coward, M. & Dietrich, D., 1989. Alpine tectonics—an overview, in *Alpine Tectonics,* pp. 353–367, eds Coward, M.P., Dietrich, D. & Park, R.G., Geol. Soc. Lond. Spec. Publ. **45.**

Davy, P. & Gillet, P., 1986. The stacking of thrust slices in collision zones and its thermal consequences, *Tectonics,* **5,** 913–929.

Deichmann, N. & Baer, M., 1990. Earthquake focal depths below the Alps and northern Alpine foreland of Switzerland, in *The European Geotraverse: Integrative Studies,* pp. 277–288, eds Freeman, R., Giese, P. & Mueller, S., European Science Foundation, Strasbourg, France.

Deichmann, N. & Rybach, L., 1989. Earthquakes and temperatures in the lower crust below the northern Alpine Foreland of Switzerland, in *Properties and Processes of the Earth's Lower Crust,* pp. 197–213, eds Mereu, R.F., Mueller, S. & Fountain, D.M., Am. Geophys. Union, Geophys. Monogr, **51.**

Dewey, J.F., Helman, M.L., Turco, E., Hutton, D.H.W. & Knott, S.D., 1989. Kinematics of the western Mediterranean, in *Alpine tectonics,* pp. 353–367, eds Coward, M.P., Dietrich, D. & Park, R.G., Geol. Soc. Lond. Spec. Publ. **45.**

England, P.C., 1978. Some thermal considerations of the Alpine metamorphism—past, present and future, *Tectonophysics,* **46,** 21–40.

Freeman, R., Kissling, E., Rasa, W., Mueller, S. & Okaya, N., 1995. *Thermomechanical behaviour of the crust–mantle system in the Central Swiss Alps,* p. B6, IUGG XXI General Assembly, Boulder, CO, (abstract).

Frey, M., Bucher, K., Frank, E. & Mullis, J., 1980. Alpine metamorphism along the Geotraverse Basel–Chiasso: A review, *Eclog. geol. Helv.,* **73,** 527–546.

Geiger, A., Kahle, H.-G. & Gubler, E., 1986. Recent crustal movements in the Alpine–Mediterranean region analyzed in the Swiss Alps, *Tectonophysics,* **130,** 289–298.

Giese, P., 1970. Die Temperaturverteilung in der Erdkruste des Alpenvorlandes und der Alpen, abgeschätzt aus tiefenseismischen Beobachtungen, *Schweiz. Min. Petrogr. Mitt.,* **48,** 597–610.

Gubler, E., 1976. Beitrag des Landesnivellements zur Bestimmung vertikaler Krustenbewegungen in der Gotthard-Region, *ICG Sci. Rept,* **37,** 675–678.

Gubler, E., 1991. Swiss National Levelling Net, in *Report on the Geodetic Activities in the Years 1988–1991,* XIX General Assembly, Int. Un. Geod. Geophys. Vienna.

Gubler, E., Arca, S., Kakkuri, J. & Zippelt, K., 1992. Recent vertical crustal movements, in *A Continent Revealed: The European Geotraverse, Atlas of Compiled Data,* pp. 20–24, eds Freeman, R. & Mueller, S., Cambridge University Press, Cambridge.

Holliger, K. & Kissling, E., 1992. Gravity interpretation of a unified 2-D acoustic image of the central Alpine collision zone, *Geophys. J. Int.,* **111,** 213–225.

Hunziker, J.C., Desmons, J. & Martinotti, G., 1989. Alpine thermal evolution in the central and western Alps, in *Alpine tectonics,* pp. 353–367, eds Coward, M.P., Dietrich, D. & Park, R.G., Geol. Soc. Lond. Spec. Publ. **45.**

Hurford, A.J., Flisch, M. & Jäger, E., 1989. Unravelling the thermotectonic evolution of the Alps: a contribution from fission track analysis and mica dating, in *Alpine Tectonics,* pp. 369–398, eds Coward, M.P., Dietrich, D. & Park, R.G., Geol. Soc. Lond. Spec. Publ. **45.**

Kissling, E., Mueller, S. & Werner, D., 1983. Gravity anomalies, seismic structure and geothermal history of the Central Alps, *Ann. Geophys.,* **1,** 37–46.

Laubscher, H., 1990. The deep structure of the Alps inferred from both geophysical and geological data, *Terra Nova,* **2,** 645–652.

Laubscher, H., 1991. The arc of the Western Alps today, *Eclog. geol. Helv.,* **84,** 631–659.

Molnar, P. & England, P., 1990. Temperatures, heat flux, and frictional stress near major thrust faults, *J. geophys. Res.,* **95,** 4833–4856.

Mueller, S., 1990. Intracrustal detachment and wedging along a detailed cross section in central Europe, in *Exposed Cross-Sections of the Continental Crust,* pp. 623–643, eds Salisbury, M.H. & Fountain, D.M., Kluwer Academic Publishers, Dordrecht, The Netherlands.

Okaya, N., 1993. Zweidimensionale thermo-kinematische Modellberechnungen zu Problemen der Kontinent–Kontinent-Kollissionstektonik am Beispiel der Schweizer Alpen (EGT), *PhD thesis,* Swiss Federal Institute of Technology (ETH), Zurich, Switzerland.

Okaya, N., Cloetingh, S. & Mueller, S., 1996. A lithospheric cross section through the Swiss Alps: Constraints on the mechanical structure of a continent–continent collision zone, *Geophys. J. Int.,* submitted.

Panza, G.F., Mueller, S. & Calcagnile, G., 1980. The gross features of the lithosphere–asthenosphere system in Europe from seismic surface waves and body waves, *Pure appl. Geophys.,* **118,** 1209–1213.

Pavoni, N., 1980. Crustal stress inferred from fault-plane solutions of earthquakes and neotectonic deformation in Switzerland, *Rock Mechanics,* Suppl., **9,** 63–68.

Peaceman, D.W. & Rachford, H.H., 1955. The numerical solution of parabolic and elliptic differential equations, *J. Soc. Ind. appl. Math.,* **3,** 28–41.

Pfiffner, A., 1992. Alpine orogeny, in *A Continent Revealed: The European Geotraverse,* pp. 180–190, eds Blundell, D., Freeman, R. & Mueller, S., Cambridge University Press, Cambridge.

Rybach, L., Werner, D., Mueller, S. & Berset, G., 1977. Heat flow, heat production and crustal dynamics in the central Alps, Switzerland, *Tectonophysics,* **41,** 113–126.

Schatz, J.F. & Simmons, G., 1972. Thermal conductivity of Earth materials at high temperatures, *J. geophys. Res.,* **77,** 6966–6983.

Schoenborn, G., 1992. Alpine tectonics and kinematic models of the central Southern Alps, *Mem. Sci. Geol., Padova,* **44,** 229–393.

Stacy, F.D., 1977. A thermal model of the Earth, *Phys. Earth planet. Inter.,* **15,** 341–348.

Stampfli, G.M., 1993. Le Briançonnais, terrain exotique dans les Alpes?, *Eclog. geol. Helv.,* **86,** 1–45.

Suhadolc, P., Panza, G.F. & Mueller, S., 1990. Physical properties of the lithosphere–asthenosphere system in Europe, *Tectonophysics,* **176,** 123–135.

Thompson, A.B., 1992. Metamorphism and fluids, in *Understanding the Earth,* pp. 222–248, eds Brown, G.C., Hawkesworth, C.J. & Wilson, R.C.L., Cambridge University Press, Cambridge.

Trümpy, R., 1973. The timing of orogenic events in the central Alps, in *Gravity and Tectonics,* pp. 229–251, eds DeJong, K.A. & Scholten, R., John Wiley & Sons, New York, NY.

Trümpy, R., 1982. Alpine paleogeography: a reappraisal, in *Mountain Building Processes,* pp. 149–156, ed. Hsü, K.J., Academic Press, London.

Valasek, P., Mueller, S., Frei, W. & Holliger, K., 1991. Results of NFP 20 seismic reflection profiling along the Alpine section of the European Geotraverse (EGT), *Geophys. J. Int.,* **105,** 85–102.

van den Beukel, J.P., 1989. Thermal and mechanical modeling of convergent plate margins, *PhD thesis,* University of Utrecht, The Netherlands.

Werner, D., 1980. Probleme der Geothermik im Bereich der Schweizer Zentralalpen, *Eclog. geol. Helv.,* **73,** 513–525.

Werner, D., 1981. A geothermic method for the reconstruction of the uplift history of a mountain range, applied to the Central Alps, *Geol. Runds.,* **70,** 296–301.

Werner, D., 1986. Paleotemperatures in the Central Alps—an attempt at interpretation, in *Lecture Notes in Earth Sciences, 5,*

Paleogeothermics, pp. 185–193, eds Buntebarth, G. & Stegena, L., Springer–Verlag, Berlin, Heidelberg.

Werner, D. & Kissling, E., 1985. Gravity anomalies and dynamics of the Swiss Alps, *Tectonophysics,* **117,** 97–108.

Werner, D., Köppel, V., Hänny, R. & Rybach, L., 1976. Cooling models for the Lepontine area (Central Swiss Alps), *Schweiz. min. petrogr. Mitt.,* **56,** 661–667.

Wyllie, P.J., 1987. Transfer of subcratonic carbon into kimberlites and rare earth carbonatites, in *Magmatic Processes: Physiochemical principles,* pp. 107–119, ed. Mysen, B.O., Spec. Publ. 1, Geochemical Society, University Park, Pennsylvania, PA.

Ye, S., 1992. Crustal structure beneath the central Swiss Alps derived from seismic refraction data, *PhD thesis,* Swiss Federal Institute of Technology (ETH), Zurich, Switzerland.

Ye, S., Ansorge, J., Kissling, E. & Mueller, S., 1990. Crustal structure beneath the eastern Swiss Alps derived from seismic refraction data, *Tectonophysics,* **242,** 119–121.

Zoth, R. & Haenel, G., 1988. Thermal Conductivity, in *Handbook of Terrestrial Heat Flow Density Determinations,* pp. 449–466, eds Haenel, R., Rybach, L. & Stegena, L., Kluwer Academic Publishers, Dordrecht, The Netherlands.

APPENDIX A: ROCK PARAMETERS USED IN THE THERMOKINEMATIC CALCULATIONS

To describe the changing thermal properties with depth, a differentiation in crust, lithospheric mantle and sublithospheric mantle is considered. Within each layer, the thermal conductivity and specific heat capacity are temperature-dependent; the radiogenic heat production in the crust is depth-dependent and in the mantle is constant. The density is constant in both crust and mantle, with different values, where the crustal density, ρ_C, is 2800 kg m^{-3} and the mantle density, ρ_M, is 3300 kg m^{-3}. The volume expansion coefficient $\alpha = 30 \times 10^{-6}\,1\,°C^{-1}$. To derive the temperature dependence of the thermal conductivity and the specific heat capacity we assumed a generalized petrological structure represented by a crust changing with depth from felsic to mafic composition, and an ultramafic mantle.

The temperature dependence of the thermal conductivity of the crust K_C is based on Zoth & Haenel (1988). Here we combine the temperature dependences of acid upper-crustal material and mafic lower-crustal material. The derived equation is

$$K_C[\mathrm{Wm^{-1}\,K^{-1}}] = \frac{532.6}{267.1 + \mathrm{T[°C]}} + 0.86. \tag{A1}$$

For the mantle lithosphere we chose a thermal conductivity model (K_M) according to Schatz & Simmons (1972). It is given by the sum of the lattice conductivity KL_M and the radiative conductivity KR_M:

$$K_M = KL_M + KR_M, \tag{A2}$$

where

$$KL_M[\mathrm{Wm^{-1}\,K^{-1}}] = \frac{418.68}{31 + 0.21(\mathrm{T[°C]} + 273)}, \tag{A3a}$$

$$KR_M[\mathrm{Wm^{-1}\,K^{-1}}] = 0 \qquad \mathrm{T} < 230\,°\mathrm{C}, \tag{A3b}$$

$$KR_M[\mathrm{Wm^{-1}\,K^{-1}}] = 2.303 \times 10^{-3}(\mathrm{T[°C]} - 227) \qquad \mathrm{T} \geq 230\,°\mathrm{C}. \tag{A3c}$$

The thermal conductivity in the sublithosphere, K_{art}, is taken according to Okaya (1993):

$$K_{art}(T) = K_0 \frac{1}{0.5\pi} \times \arctan[K_1(T - T_{art} - \Delta T) + K_M(T_{art}) + \Delta K], \tag{A4}$$

where

$$\Delta K = \frac{\tan(0.7 \times 0.5\pi)}{K_1}, \tag{A5a}$$

$$\Delta T = 0.7K_0. \tag{A5b}$$

The temperature dependence of the specific heat capacity in the crust cp_C is (England 1978):

$$cp_C[\mathrm{J\,kg^{-1}\,°C^{-1}}] = 786 + 0.4264(\mathrm{T[°C]} + 273) - \frac{1.3327 \times 10^7}{(\mathrm{T[°C]} + 273)^2}. \tag{A6}$$

A good estimate for the specific heat capacity in the mantle cp_M is 1250 J kg^{-1} °C^{-1} (Stacy 1977). The specific heat capacity in the sublithosphere, cp_{art}, is chosen to be 10^6 J kg^{-1} °C^{-1}. It is generally recognised that heat production on a crustal scale decreases with increasing depth. However, the precise form of this relationship is unknown and varies locally. An exponential decrease with depth is compatible with observations,

$$A_C[\mu\mathrm{W\,m^{-3}}] = A_0 \exp\left(-\frac{z}{D}\right), \tag{A7}$$

where A_0 is the radiogenic heat production at the surface, z is the depth and D_0 is a parameter with the dimension of length characterising the decrease of the radiogenic heat production with depth. For A_0 we chose the value of 2.8 μW m^{-3}, which is typical for granite (Cermák & Rybach 1982). The parameter D_0 is parametrized via the surface heat flow Q_S by using the empirical relation (e.g. Chapman & Pollack 1977; Chapman 1986)

$$0.4Q_S = A_0 D_0. \tag{A8}$$

For D_0 we obtained 10 km assuming a surface heat flow, Q_S, of 70 mW m^{-2}.